Journal of Inclusion Phenomena and Macrocyclic Chemistry **35:** 431–449, 1999.

Inclusion Compounds Formed by Triphenylmethanol: Structure, Guest Dynamics and Thermal Stability

KARIN ECKARDT[1], HELMUT PAULUS[1], HARTMUT FUESS[1,⋆], NORIKO ONODA-YAMAMURO[2], RYUICHI IKEDA[2] and ALARICH WEISS†
[1]*Materials Science Department, Darmstadt University of Technology, Petersenstraße 23, D-64287 Darmstadt, Germany;* [2]*Department of Chemistry, University of Tsukuba, Tsukuba, Ibaraki 305, Japan*

(Received: 9 January 1998; in final form: 12 January 1999)

Abstract. The crystal structure of an inclusion compound formed by triphenylmethanol with dimethylformamide was determined (space group P1 with a = 898.8(3) pm, b = 1022.3 pm, c = 1177.3 pm, α =104.57(1)°, β = 110.32(1)°, γ = 96.76(1)°, Z = 2 at T = 300 K). The structure of compounds formed with acetone and dimethylsulfoxide were rerefined. A new assignment for the acetone compound in space group $P2_1/n$ allowed a better ordered description of the molecule. The structure of the dimethylsulfoxide compound at 100 K did not indicate a phase transition and reproduced basically the room temperature structure.

The results were compared with the known structures of clathrates formed by triphenylmethanol with methanol and 1,4-dioxane. All triphenylmethanol inclusion compounds are unstable, and therefore their decomposition during heating was analysed by both thermalanalysis and X-ray powder diffraction. Vapor pressure measurements of the inclusion compounds were performed from 283 to 376 K. For the pure host no marked vapor pressure was detected in this temperature range with the setup used. From the logarithmic plots of vapor pressures versus temperature the heats of vaporization were determined. The dynamics of the deuterated guest molecules were studied by measurement of the temperature dependence of the ^{2}H NMR signals derived from powder spectra in the range 120–335 K.

Key words: Triphenylmethanol, inclusion, structure, ^{2}H NMR, dynamics, thermal stability.

Supplementary Data relating to this article (X-ray crystallographic data for the three compounds listed in Table I including tables of atomic coordinates, temperature factors, bond distances and angles, intermolecular contacts and deviations from the best planes of molecules, figures of DTA/TG traces in depence of temperature and X-ray diffractograms at selected temperatures recorded during the decomposition of compounds (**1**)–(**5**)) are deposited with the British Library as Supplementary Publication No. SUP. (19 pages)

⋆ Author for correspondence: Prof. Dr. H. Fuess, Fachbereich Materialwissenschaft der Technischen Universität Darmstadt, Petersenstraße 23, 64287 Darmstadt
Tel.: 06151/162298; Fax: 06151/166023; E-mail: dd9n@hrzpub.tu-darmstadt.de
† Deceased.

1. Introduction

Triphenylmethanol, Ph_3COH, strongly tends to include solvent molecules when crystallized from solution. The inclusion phenomena with acetone and CCl_4 were described by Norris [1] and structures of inclusion compounds formed with methanol, $Ph_3COH{\cdot}CH_3OH$, and with dimethylsulfoxide (DMSO), $2Ph_3COH{\cdot}(CH_3)_2SO$, are reported by Weber et al. [2]. Furthermore, Bourne et al. determined the structure of an inclusion compound with 1,4-dioxane as guest, $Ph_3COH{\cdot}C_4H_8O_2$ [3]. Recently Weber et al. [4] reported on further triarylmethanol host compounds and published the crystal structures of three inclusion compounds. In particular the authors described the compound formed with acetone as a guest and assigned it the monoclinic space group C2/c.

Our own investigation on the acetone compound has been carried out independently [5] in the frame of a more general study of bulky organic molecules which was focused on their property to encapture gas or solvent molecules in their crystal lattices. In a previous work we investigated clathrates of hexaphenylditin with various aromatic solvents ($Ph_6Sn_2{\cdot}2X$, X = benzene, toluene, fluorobenzene, chlorobenzene, aniline) by structure determination, vapor pressure measurements and solid state ^2H NMR spectroscopy [6].

Here we present the crystal structures of inclusion compounds formed by triphenylmethanol with acetone, $2Ph_3COH{\cdot}(CH_3)_2CO$ (**1**), dimethylsulfoxide (DMSO), $2Ph_3COH{\cdot}(CH_3)_2SO$ (**2**) and dimethylformamide (DMF), $Ph_3COH{\cdot}(CH_3)_2NCHO$ (**3**), their vapor pressures and in addition, those of inclusion compounds formed by triphenylmethanol with methanol, $Ph_3COH{\cdot}CH_3OH$ (**4**), and dioxane, $Ph_3COH{\cdot}C_4H_8O_2$ (**5**). The structure determination [4] of (**1**) has been published after completion of our work [5] whereas the reported room temperature structure of (**2**) was repeated at 100K in order to provide a basis for the interpretation of low temperature NMR-data. Based on the instability of compounds (**1**)–(**5**), the decomposition processes were investigated by both thermal analysis (DTA/TG) and X-ray powder diffraction. ^2H NMR spectroscopy was applied to study the motions of the guest molecules in the different host lattices.

2. Experimental Section

Crystal preparation. Small crystals were grown by cooling solutions of commercial Ph_3COH in the appropriate solvents. They were used for DTA/TG, X-ray diffraction and vapor pressure measurements. For ^2H NMR experiments, triphenylmethanol was crystallized from partially or fully deuterated, commercially available solvents; the samples were dried and sealed in glass tubes of 10 mm outer diameter and 20 mm length.

Thermal analysis. A SETARAM TGA 92 device was used for DTA/TG measurements in the range 295–473 K with a heating/cooling rate of 3 K/min and a dry argon stream as purge gas at a flow rate of 2 L/h. The crystals were removed from

their mother liquors directly before thermal analysis, dried on a filter paper and crushed. Sample weights were around 35 mg.

X-ray diffraction. For structure determination, single crystals were fixed and sealed in glass tubes with a small amount of mother liquor to avoid decomposition. Intensities were collected on a Stoe Stadi4 four-circle diffractometer using graphite-monochromated MoKα radiation. For data collection at 100 K the crystal was cooled using an Oxford Cryostream Cooler. The structures were determined by direct methods, Fourier analysis, and least squares refinement on F^2 [7]. All H-atom positions were derived from difference Fourier maps and refined.

For decomposition experiments, the crystals were pulverized and filled in open glass tubes, allowing slow evaporation of the solvents. A series of X-ray powder data were recorded in Debye–Scherrer geometry with a stationary position sensitive detector ($10 \leq 2\theta/^\circ \leq 50$) on a Stoe Stadip diffractometer using graphite monochromated CuKα_1 radiation. Powder diffractograms were recorded from 298 to 333 K in steps of 5 K. The temperatures were adjusted at intervals of 30 minutes between each measurement. For compound (**1**) the temperature was increased in steps of 1 K in the range 323–328 K.

Vapor pressure measurements. Crystals removed from the mother liquor were dried on a filter paper and used directly for vapor pressure measurements. Experiments were performed by a pressure gauge method [8] in the range 283–376 K. The pressure gauge made from aluminium was placed inside an evacuated aluminium vessel which was isolated from the atmosphere. Temperature control was achieved by connection with a methanol cryostat and temperature was measured by a NiCr/Ni-thermocouple. No temperature gradient has been observed along the pressure gauge.

^{2}H NMR spectroscopy. ^{2}H NMR spectra of the deuterated guest molecules in compounds (**1**)–(**4**) were measured at a Larmor frequency of 46.1 MHz using a Bruker MSL-300 spectrometer equipped with a VT-100 temperature controller. The spectra were generated by applying the quadrupole echo sequence using 90° pulses with widths of 4.5–10 μs between 120 K and 335 K.

3. Results and Discussion

3.1. CRYSTAL STRUCTURES

Ph_3COH was crystallized by cooling crystallization from methanol, diethylether, benzene, toluene, $CHCl_3$, THF, furan and DMF. The powder diffractograms of the crystals obtained were compared with the powder pattern of pure Ph_3COH having a trigonal structure, space group $R\bar{3}$ [9]. Only crystals obtained from DMF showed a powder pattern different from that of the pure host compound, indicating the existence of a new inclusion compound with a host/guest ratio of 1 : 1 derived by single crystal structure analysis. The experimental conditions for structure determination

Table I. Experimental conditions, crystal data and structure refinement for inclusion compounds (**1**)–(**3**). Diffractometer Stoe Stadi4; wavelength: (MoKα) 71.073 pm; monochromator: graphite (002), scan: $2\theta/\omega$.

	(**1**)	(**2**)	(**3**)
Empirical formula	$C_{41}H_{38}O_3$	$C_{40}H_{38}O_3S$	$C_{22}H_{23}NO_2$
Formula weight (g/mol)	578.79	598.79	334.46
Temperature (K)	299(2)	100(5)	300(2)
Crystal system	Monoclinic	Monoclinic	Triclinic
Space group	$P2_1/n = C_{2h}^5$	C2/c = C_{2h}^6	$P\bar{1} = C_i^1$
Formula units	$Z = 4$	$Z = 4$	$Z = 2$
Unit cell dimensions (pm, °)	a = 865.4(3)	a = 1615.3(6)	a = 898.8(3)
	b = 1618.6(6)	b = 858.8(3)	b = 1022.3(3)
	c = 2310.4(8)	c = 2265.2(7)	c = 1177.3(3)
			α = 104.57(1)
	β = 97.44(2)	β = 95.98(2)	β = 110.32(1)
			γ = 96.76(1)
Volume (10^{-6} pm^3)	3209(2)	3125(2)	956.4(5)
ρ_{calc} (Mg m^{-3})	1.198(1)	1.273(1)	1.158(1)
Reflections collected	8713	5435	3119
Independent Reflections	5658	2730	2495
Data/parameters	5635/550	2725/281	2487/319
$F_{(000)}$	1232	1272	356
GOF	1.163	1.218	1.130
$R_{(I>2\sigma(I))}$ (%)	R = 4.70,	R = 6.96,	R = 3.68,
	R_w = 14.11	R_w = 24.09	R_w = 12.11
R (all data) (%)	R = 7.98,	R = 8.05,	R = 5.03,
	R_w = 17.57	R_w = 25.95	R_w = 14.38

and refinement, and the crystallographic data for inclusion compounds (**1**)–(**3**) are listed in Table I.

For (**1**) the space group C2/c was suggested by Weber et al. [2], but we found additional weak reflections reducing the symmetry to space group $P2_1/n$. Thus, the compound crystallizes in the monoclinic space group $P2_1/n$ with four formula units in the cell. As the DMSO molecule differs only by one atom (substitution of a C-atom by sulphur) we reexamined the structure of (**2**) at room temperature and confirmed the space group C2/c and the lattice constants of Weber et al. [2]. No phase transition was observed by slowly cooling down to 100 K and data for a redetermination of the crystal structure of the DMSO clathrate (**2**) were collected. Due to volume contraction the lattice constants at 100 K are slightly smaller compared to those at room temperature [2]. All compounds have in common the formation of

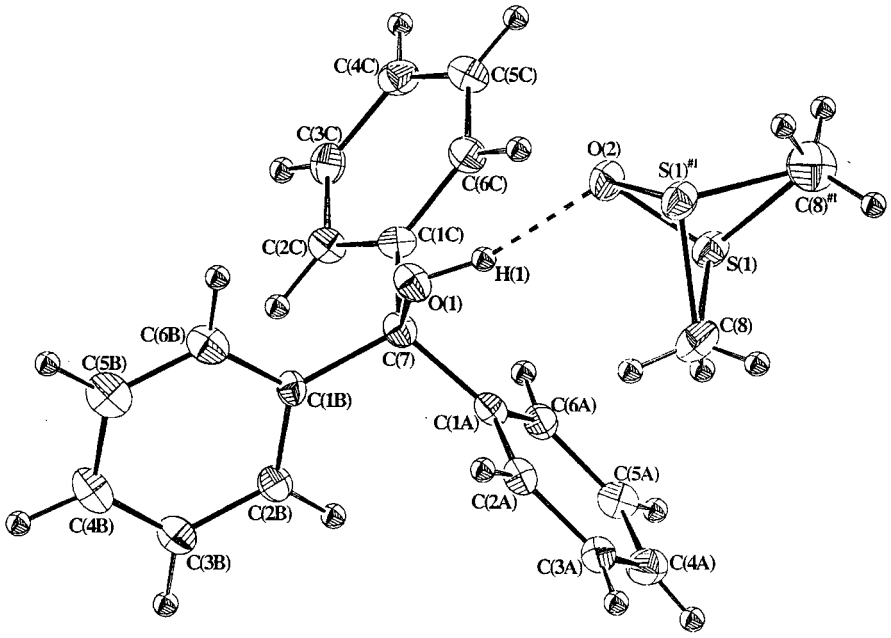

Figure 1. Molecular structure of $2Ph_3COH{\cdot}(CH_3)_2SO$ (**2**) (thermal ellipsoids at 50% probability level) at 100 K. The DMSO molecule is disordered taking two equivalent positions about the crystallographic twofold axis. Hydrogen bonds are shown by dashed lines. Atoms generated by symmetry operation $(1 - x, y, 0.5 - z)$ are marked by (#1).

hydrogen bonds between host and guest molecules. The hydrogen bond schemes are listed in Table II. The molecular structures of (**2**) and (**3**) with atoms drawn as thermal ellipsoids and hydrogen bonds marked out as dashed lines are shown in Figures 1 and 2 respectively.

In the asymmetric unit of (**1**) two host molecules and one guest are joined together into a trimer unit (Figure 3). One Ph_3COH forms a hydrogen bond to the other Ph_3COH molecule, which fixes the acetone molecule by another hydrogen bridge. In (**2**) only one half of the formula unit $2Ph_3COH{\cdot}(CH_3)_2SO$ is located in the asymmetric unit with the guest molecule being positionally disordered: oxygen atom O(2) lies on the special position (0, y, 1/4), while the point position of the sulphur atom S(1) is general, but only half-occupied by atoms. Furthermore, one methyl group of the guest molecule lies on a fully occupied general position, generating the second methyl group by twofold symmetry. Nearly the same arrangement of the atoms was described for this compound at room temperature [2]. The authors have localized two methyl C-atoms on general positions, but with a site occupancy of 1/2. Although this is only a small difference between the arrangement of the guest molecules at 100 K and room temperature it becomes essential for the interpretation of the ^2H NMR results given below. The disordered guest molecule is inserted between two host molecules, being able to form a hydrogen

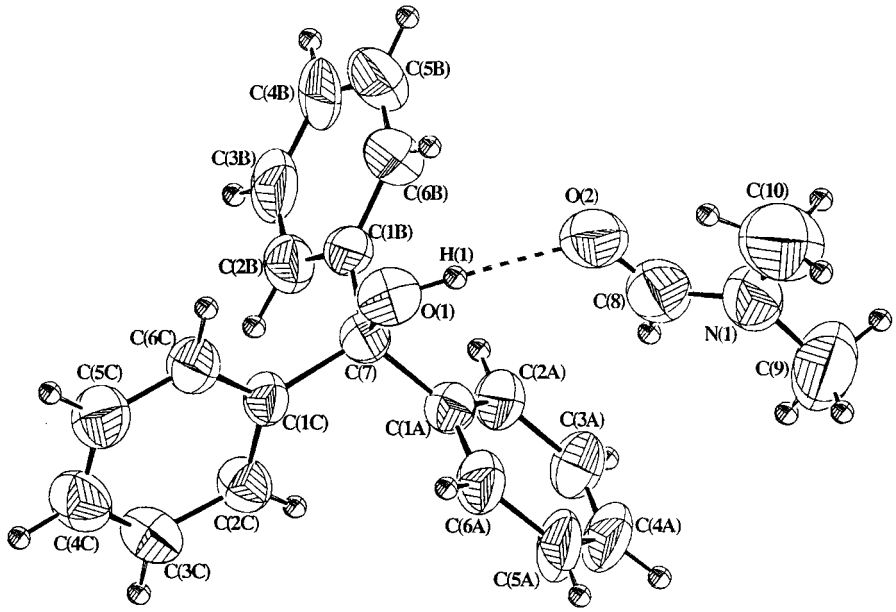

Figure 2. Molecular structure of $Ph_3COH{\cdot}(CH_3)_2NCHO$ (**3**) (thermal ellipsoids at 50% probability level). Hydrogen bonds are marked out as dashed lines.

bond to either one. In contrast to the acetone compound, no hydrogen bond between host molecules is formed in (**2**) as can be seen from the nearest distance between the hydroxy oxygen atoms of two neighbouring triphenylmethanol molecules of 445.4 pm, which is greater than the sum of their van der Waals radii [10]. Different sizes and shapes of the guest molecules may contribute to that behaviour: acetone is smaller and the skeleton is planar therefore allowing an interaction between adjacent host molecules, while the size of DMSO is increased by the sulphur atom and its free electron pair, inducing a nonplanar shape of the guest. Furthermore DMSO is a much stronger proton acceptor than acetone and therefore it attracts more easily two proton donating groups from neighboring hosts and prevents them from H-bonding, to each other.

In the DMF compound (**3**) again the hydroxy group of the host molecule is connected to the oxygen atom of the guest molecule by a hydrogen bond and no “strong” interaction between host molecules is found. A similar connection is reported for the dioxane compound $Ph_3COH{\cdot}C_4H_8O_2$ (**5**) [3], while in the methanol clathrate $Ph_3COH{\cdot}CH_3OH$ (**4**) two host and two guest molecules are linked together into a tetrameric unit by a circular hydrogen bond scheme with hydrogen bonds alternating from host to guest [2]. The packing of the molecules in the crystal lattices is indicated for compounds (**1**) and (**3**) by the projections of the unit cells shown in Figures 3 and 4 respectively. The structures of clathrates (**1**)–(**3**) as well as (**4**) and (**5**) all have in common the formation of bilayers interacting by van der Waals forces. The centres of these layers are formed by the polar groups of the

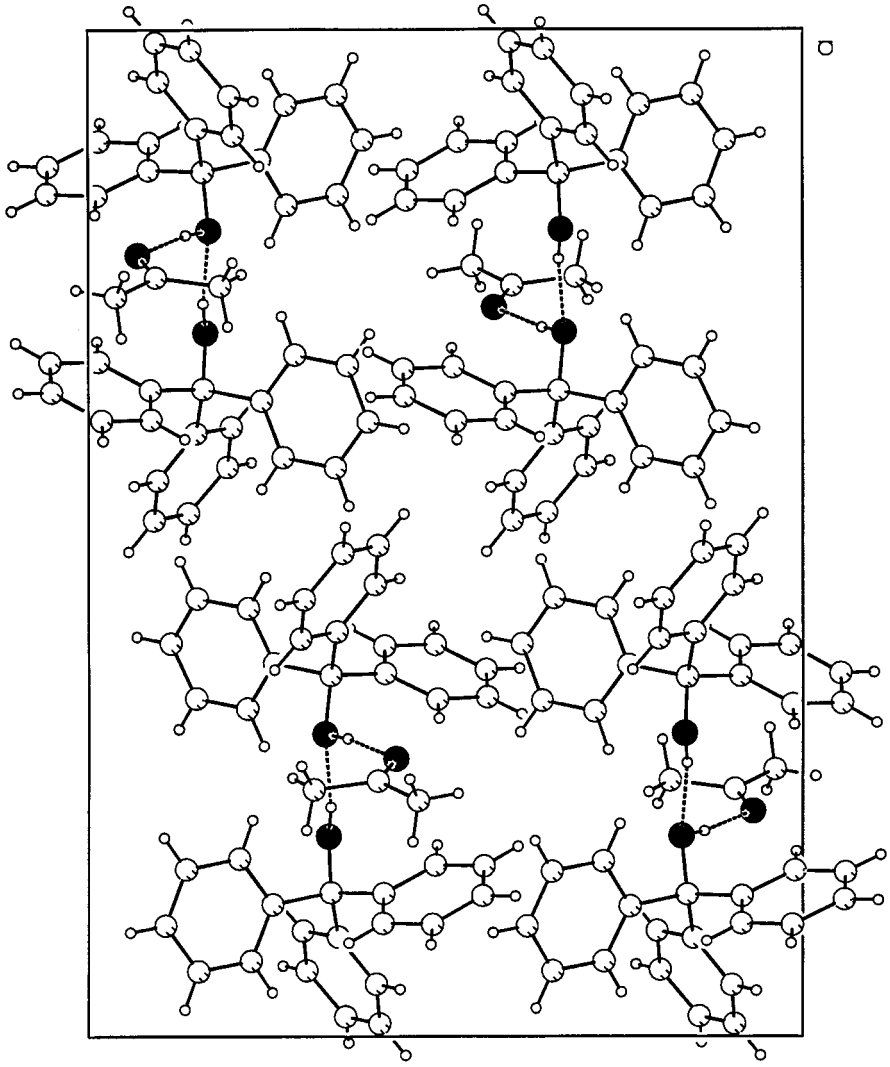

Figure 3. Projection of the unit cell of $2Ph_3COH{\cdot}(CH_3)_2CO$ (**1**) along [1 0 0]. Hydrogen bonds are marked out as dashed lines.

guests and hydroxy groups of triphenylmethanol molecules and enveloped by the less polar phenyl rings of the host molecules. Thus guest molecules are surrounded and shielded by the large phenyl substituents of the host molecules. For all five compounds the bilayers are parallel to the *ab*-plane.

The bond lengths and angles of the triphenylmethanol molecules in compounds (**1**)–(**3**) lie within the expected ranges, worthy of mention is a slight narrowing of the C-C-C-angle at the substitution point of the phenyl rings and a small widening at the opposite carbon atom as observed also for a number of naphthalene derivatives [11].

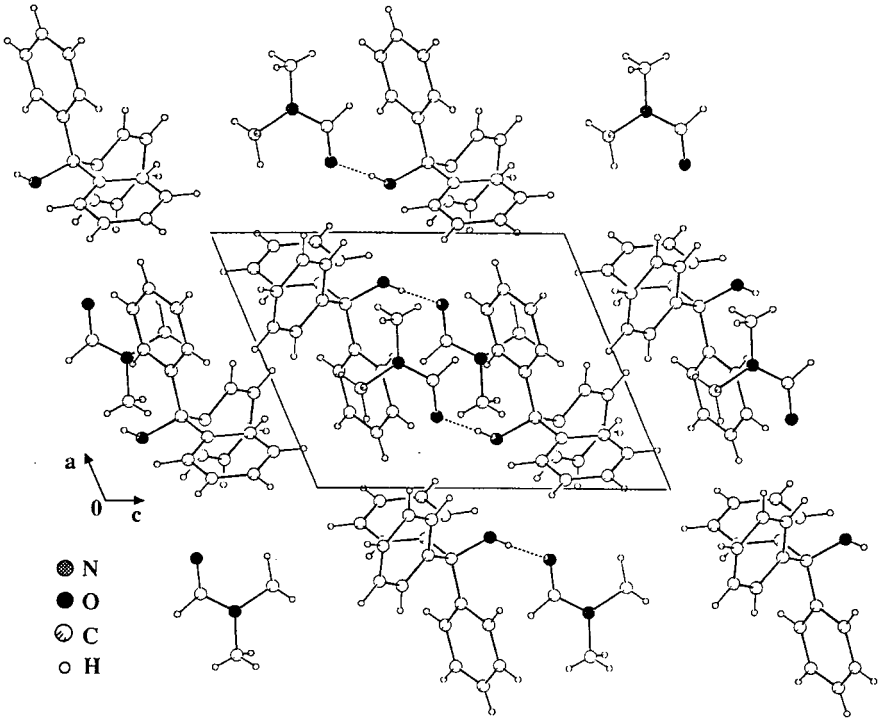

Figure 4. Projection of the structure of $Ph_3COH{\cdot}(CH_3)_2NCHO$ (**3**) along [0 1 0] ($0 \leq x \leq 1$, $-0.5 \leq y \leq 1.5$, $-0.5 \leq z \leq 1.5$) Hydrogen bonds are marked out as dashed lines.

^{2}H NMR spectra

*$2Ph_3COH{\cdot}(CD_3)_2CO$ (**1**).* In Figure 5 the ^{2}H NMR spectra of $2Ph_3COH{\cdot}(CD_3)_2CO$ (**1**) recorded at different temperatures from 120 to 325 K are shown, while the determined values of quadrupole coupling constants (qcc), e^2qQh^{-1}, and η are listed in Table III. The qcc value of 54.3 kHz observed at 120 K can be well explained by the model of CD_3 reorientation about the C—C bond. This motion results in 1/3 of the qcc value for a rigid CD_3 group reported as 165–175 kHz [12], provided tetrahedral bond angles in a methyl group are assumed. The large η value of 0.17 is exceptional in a rotating CD_3 group suggesting the presence of anisotropic interactions in the crystals at low temperatures. A similar value for η of 0.14 was reported for crystalline $(CD_3)_2CO$ at low temperatures [13]. Upon heating, the spectra are narrowed and the asymmetry of the electric field gradient is increased. The sharp peak occuring above 280 K in the centre of the spectra is attributed to liquid guest molecules liberated from the inclusion compound. The lineshape observed at 325 K indicates the onset of a new reorientational motion. From the pronounced asymmetry of the spectrum we expect two-site jumps of both CD_3 groups of the guest molecule. The qcc and η values determined at 325 K require possible jump angles of 55.0° and 125°, which were evaluated according

Table II. Hydrogen bond scheme (bond lengths (pm) and angles (°))

Compound	Connection	Bond, angle	T (K)
(**1**)	O(1)···O(2)	285.0 pm	299
	O(1)—H(1)···O(2)	168.4°	
	O(2)···O(3)	274.0 pm	
	O(2)—H(2)···O(3)	173.7°	
(**2**)	O(1)···O(2)	281.2 pm	100
	O(1)—H(1)···O(2)	163.0°	
	O(1)···O(2)*	284.2 pm	≈300
	O(1)—H(1)···O(2)*	170°	
(**3**)	O(1)···O(2)	280.3 pm	300
	O(1)—H(1)···O(2)	174.8°	
(**4**)	O(1)···O(2)*	270.7 pm	≈300
	$O(1)^{\#}$···O(2)*	272.1 pm	
	O(1)—H(1)···O(2)*	170°	
(**5**)	O(1)···O(2)	285.5 pm	304
	O(1)—H(1)···O(2)	160.5°	

to Ikeda et al. [14] by assuming $\eta \approx 0.0$ for the rigid state. Since the latter angle is close to the C—C—C bond angle of 117.5° determined by X-ray diffraction, this new motion is assigned to the 180°-flip about the molecular C_2-axis. Despite this motion the atomic positions of the guest molecules are well defined, which is consistent with the present X-ray results. The smaller value of the structural bond angle compared to the jump angle estimated from the ^{2}H NMR spectrum at 325 K arises from enhanced thermal motion of the methyl carbon atoms in acetone.

*$2Ph_3COH{\cdot}(CD_3)_2SO$ (**2**).* ^{2}H NMR spectra of $2Ph_3COH{\cdot}(CD_3)_2SO$ (**2**) recorded between 120 and 295 K are represented in Figure 6 together with the simulated spectra discussed below. The qcc value of 56.7 kHz and $\eta = 0.0$ observed at 120 K can be explained by the model of CD_3 reorientation about the C—S bond as discussed above. As only one Pake-doublet is found we conclude that the two methyl groups of the guest molecules are equivalent at low temperature. This is consistent with the present crystal structure determination of (**2**), revealing the crystallographic equivalence of the two methyl groups of DMSO.

The sharp central line occuring above 220 K is due to desolvated guest molecules. The narrowed spectra with two pairs of satellites around the centre observed above 230 K indicate the onset of a new dynamic process. The lineshapes result from the superposition of the spectra arising from two kinds of CD_3 groups, that have nonequivalent sites and different η values but roughly the same abundance. The large η values expected from the observed lineshape imply the onset of

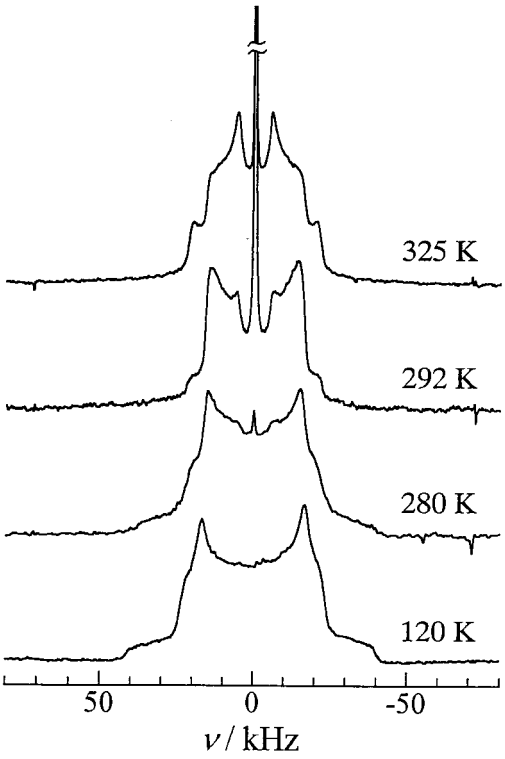

Figure 5. ^{2}H NMR spectra of $2Ph_3COH{\cdot}(CD_3)_2CO$ observed at various temperatures.

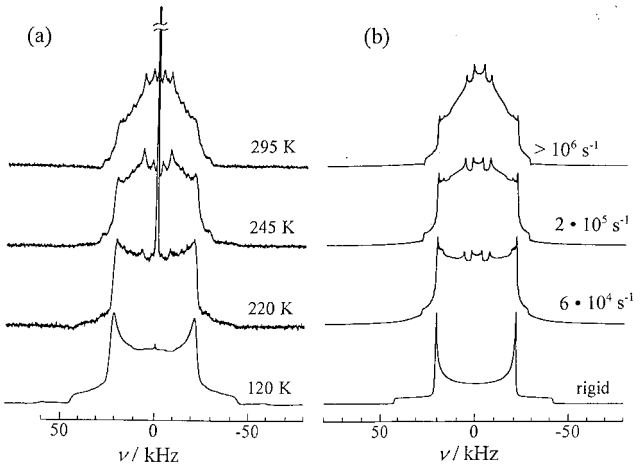

Figure 6. ^{2}H NMR spectra of $2Ph_3COH{\cdot}(CD_3)_2SO$ observed at various temperatures (a) and simulated with several jumping rates of two-site jumps for two nonequivalent CD_3 groups (b).

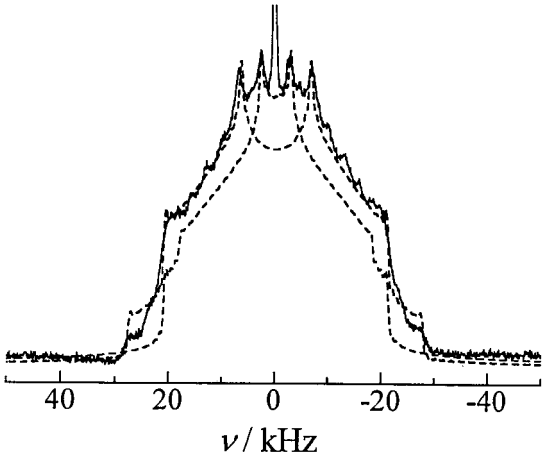

Figure 7. Separation of the ^{2}H NMR spectrum observed (solid line) in $2Ph_3COH{\cdot}(CD_3)_2SO$ at 295 K into two spectra simulated (broken line) by the two-site jump model giving e^2qQh^{-1} = 36.9 and 27.8 kHz, η = 0.53 and 0.73 and jump angles of 123 and 104° for the outer and inner spectra, respectively. Comparison with the observed spectrum should be done by reducing to one-half the simulated intensity.

two-site jumps for both of these two nonequivalent CD_3 groups [15]. We separated the spectrum observed at 295 K into two components by simulating spectra [14] for CD_3 groups performing two-site jumps by an angle of 2θ, using the values for qcc of 56.0 kHz and η = 0.0 determined at 200 K for the rigid methyl groups before the onset of jumps. The simulated lineshapes are superimposed on the observed spectrum as shown in Figure 7. The two sets of qcc and η values obtained at 295 K are given in Table III.

According to Weber et al. [2], the nonplanar guest molecules in $2Ph_3COH{\cdot}(CH_3)_2SO$ crystals occupy disordered orientations around the crystallographic two-fold axis at room temperature. In contrast to the arrangement at low temperature, the two methyl groups are not equivalent any more at room temperature. Since the carbon atoms were shown to be located in general positions, the directions of the two S—C bonds in the DMSO molecule are expected to jump between two orientations with different jump angles. From the reported structural parameters [2] we roughly evaluated the jump angles of the two S-C bonds to be 106.6° and 126.9°. These angles agree well with the derived angles of 104° and 123°, corresponding to the small and large qcc values observed at 295 K, respectively. Based on this motional model, we simulated ^{2}H NMR spectra under various jumping rates by superimposing two spectra calculated with the jump angles given above. The simulated spectra at different jumping rates corresponding to the observed spectra are shown in Figure 6b. It gives a rough impression of the dependence of the jumping rate of CD_3 groups in crystals on temperature. From these results, we conclude that at room temperature the nonplanar $(CD_3)_2SO$ molecules perform

Table III. Observed quadrupole coupling constants e^2qQh^{-1} and asymmetry parameters η of the electric field gradient at ^{2}H nuclei in $2Ph_3COH{\cdot}(CD_3)_2CO$ (**1**), $2Ph_3COH{\cdot}(CD_3)_2SO$ (**2**), $Ph_3COH{\cdot}(CD_3)_2NCDO$ (**3**) and $Ph_3COH{\cdot}CD_3COH$ (**4**).

Compound	Low temperature			High temperature		
	e^2qQh^{-1} (kHz)	η	T (K)	e^2qQh^{-1} (kHz)	η	T (K)
$2Ph_3COH{\cdot}(CD_3)_2CO$ (**1**)	54.3 ± 0.2	0.17 ± 0.01	130	29.0 ± 0.2	0.47 ± 0.01	325
$2Ph_3COH{\cdot}(CD_3)_2SO$ (**2**)	56.7 ± 0.2	0.0*	120	36.9 ± 0.4	0.53 ± 0.03	295
				27.8 ± 0.4	0.73 ± 0.03	295
$Ph_3COH{\cdot}(CD_3)_2NCDO$ (**3**)	50.9 ± 0.2	0.0*	120	47.3 ± 0.2	0.0*	300
				14.8 ± 1.0	0.0*	300
$Ph_3COH{\cdot}CD_3COH$ (**4**)	50.0 ± 0.2	0.0*	120	$47.0 \pm 0.20.0$*	300	

* Assumed.

two-site jumps about the crystallographic twofold axis on which the guest O atoms are located. This motional model agrees well with the X-ray results [2], reporting a two-site disorder of C and S atoms of the guest molecules at room temperature. The ^{2}H NMR results may indicate that the positional disorder of dimethylsulfoxide is static at low temperatures and dynamic at room temperature.

*$Ph_3COH{\cdot}(CD_3)_2NCDO$ (**3**) and $Ph_3COH{\cdot}CD_3OH$ (**4**).* No significant changes are recorded in the spectra for $Ph_3COH{\cdot}(CD_3)_2NCDO$ (**3**) and $Ph_3COH{\cdot}CD_3OH$ (**4**) at different temperatures. ^{2}H NMR spectra of both compounds at 120 K reveal lineshapes that are typical for CD_3 groups performing C_3-reorientations having an almost vanishing asymmetry parameter η and the qcc values are given in Table III. The wide and weak pair of peaks with a splitting of 112 kHz observed for (**3**) at 300 K are assigned to deuterons in the static CD_3 group. Upon heating above room temperature, the lineshapes of both compounds are basically unchanged. These results imply that no motions other than the CD_3 reorientation takes place up to room temperature in the $(CD_3)_2NCDO$ and CD_3OH compounds. This is in good agreement with the results of the present and reported [2] X-ray analysis, respectively, providing no disordered atomic arrangement of the solvent molecules at room temperature.

3.2. DECOMPOSITION EXPERIMENTS

Thermal Analysis (DTA/TG). The results of DTA/TG measurements for compounds (**1**)–(**5**) are summarized in Table IV. For sake of comparison the boiling points of the pure solvents are also given [16]. Two endothermic effects are observed for $2Ph_3COH{\cdot}(CH_3)_2CO$ (**1**), $Ph_3COH{\cdot}CH_3COH$ (**4**) and $Ph_3COH{\cdot}C_4H_8O_2$ (**5**) in DTA during heating. The first peak can be assigned to the loss of the encaptured solvent from the clathrate as concluded from the weight loss in the TG traces. The second endothermic peak can be attributed to the melting of the remaining solvent free host, being in good agreement with the melting point for pure triphenylmethanol of 436–439 K [17]. During cooling the solidification of the triphenylmethanol melt leads to one exothermic peak in DTA at temperatures of more than 50 K below the melting point. In the cases of $2Ph_3COH{\cdot}(CH_3)_2SO$ (**2**) and $Ph_3COH{\cdot}(CH_3)_2NCHO$ (**3**) only one pronounced endothermic effect is detected during heating, accompanied by a continuous weight loss caused by the liberation of guest molecules from crystal solvates. These processes are spread out over a greater temperature range than for the compounds discussed above. Again a pronounced undercooling is observed.

The experimental values for the weight loss detected by thermogravimetry correspond well with the theoretical ones, while the largest deviation of 1.85% for (**2**) is due to a small amount of mother liquor adhering to the crystals. From the TG-traces it becomes evident that the liberation of the encaptured guest molecules takes place in one step. The step-like effect observed for (**5**) above 420 K is due to

Table IV. Results of thermal analysis DTA/TG. The temperatures of the first and second endothermic peak occuring on heating and of the exothermic effect on cooling are given, together with the experimental and theoretical weight loss and the boiling points T_b of the pure solvents [14].

Compound	Heating		Cooling	Weight loss Δm		T_b
	1. Endo.	2. Endo. peak	Exo. peak	$\Delta m_{\text{exp.}}$ (%)	$\Delta m_{\text{theor.}}$ (%)	
(**1**)	335–359 K	440 K	383.5 K	−9.6	−8.77	329.3 K
(**2**)	393–420 K		385.1 K	−14.9	−13.05	462.1 K
(**3**)	344–362 K		381.3 K	−22.2	−21.93	426.0 K
(**4**)	358–382 K	440 K	384.6 K	−10.86	−10.96	337.6 K
(**5**)	356–380 K	432.3 K	384.8 K	−24.9	−25.28	374.4 K

a residue of dioxane that is expelled from the solid shortly below the melting point of triphenylmethanol.

No correlation is observed between the decomposition temperatures of the compounds and the boiling points T_b of the corresponding pure solvents. Bourne et al. [3] suggested that the functions $T_{\text{on}} - T_b$ or T_{on}/T_b, where T_{on} is the onset temperature of guest release, could be useful parameters indicating compound stability. But the boiling points depend on the interactions between the molecules in the liquid phase and are lower for solvents with weaker interactions than for liquids that e. g. form hydrogen bonds. If two guest molecules experience similar forces in the crystal lattice of the clathrate and therefore similar temperatures of guest release, T_{on}, but have strongly differing boiling points, the ratio T_{on}/T_b would lead to erroneous conclusions about clathrate stability.

X-Ray Powder Diffraction. A series of X-ray powder diffractograms were recorded during the thermal decomposition of the compounds (**1**)–(**5**). As an exemplification selected powder patterns at different temperatures for compounds (**1**) and (**3**) are shown in Figures 8 and 9, respectively. For the acetone compound we observe the diffractogram corresponding to the monoclinic modification of (**1**) at room temperature. The intensities of these reflections decrease with increasing temperature, especially in the narrow range from 323 K to 325 K. At 328 K new reflections appear, that can be indexed according to the trigonal modification of pure Ph_3COH [9]. A similar behaviour is found for the methanol clathrate, where the triclinic modification of (**4**) decomposes around 343 K to the solvent free trigonal modification of Ph_3COH. In contrast the intensities of reflections belonging to the monoclinic phase of the DMSO compound (**2**) diminish above 348 K but no other solid phase is formed at higher temperatures. A powder pattern with a high background typical for liquids is detected at 403 K. Around 333 K the tri-

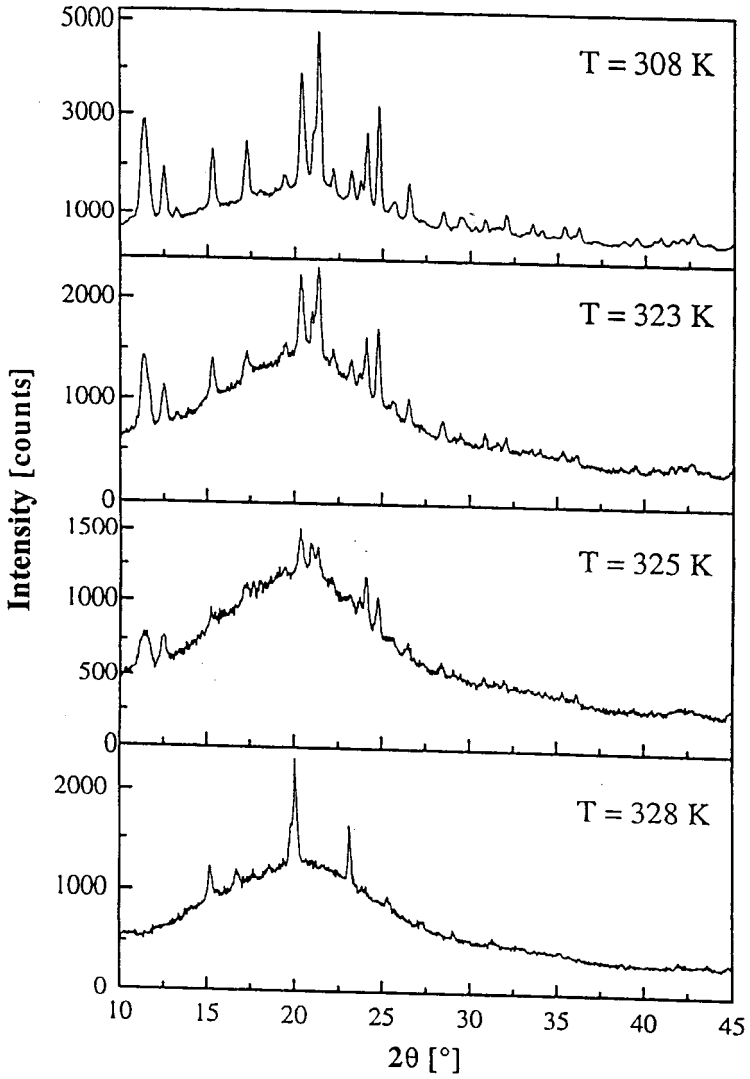

Figure 8. X-ray powder diffractograms at selected temperatures recorded during the decomposition of $2Ph_3COH{\cdot}(CH_3)_2CO$ (monoclinic $P2_1/n$) to the solvent free modification of Ph_3COH (trigonal $R\bar{3}$).

clinic phase of the DMF compound (**3**) transforms to the trigonal modification of Ph_3COH as indicated by a few weak reflections emerging from the background (Figure 9). A similar behaviour is observed for the dioxane clathrate (**5**), where a significant change in the powder patterns of the triclinic phase occurs between 343 and 368 K. At the latter temperature only a high background and few reflections resulting from pure crystalline triphenylmethanol are observed.

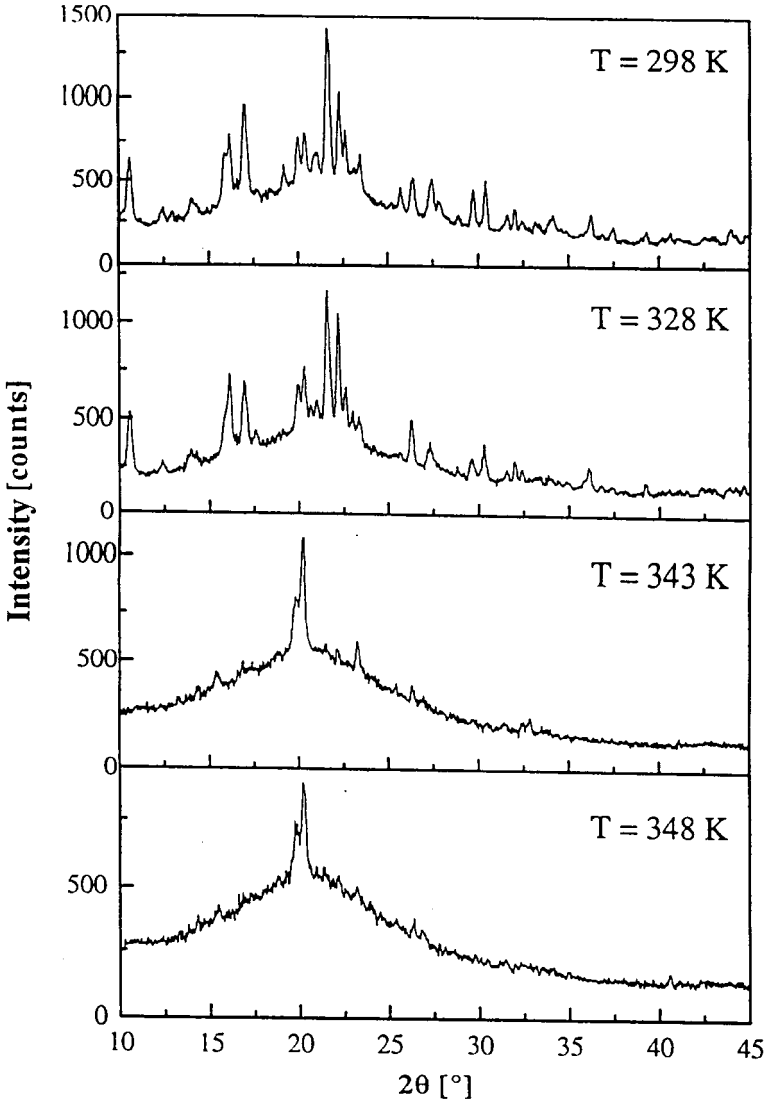

Figure 9. X-ray powder diffractograms at selected temperatures recorded during the decomposition of $Ph_3COH{\cdot}(CH_3)_2NCHO$ (triclinic $P\bar{1}$) to the solvent free modification of Ph_3COH (trigonal $R\bar{3}$).

No intermediate phase is formed during the decomposition of compounds (**1**)-(**5**) as indicated by X-ray powder diffraction experiments. After decomposition of the inclusion compounds with acetone and methanol strong reflections of the trigonal modification of triphenylmethanol are observed. This is consistent with the DTA results, where a pronounced endothermic peak at the melting point of triphenylmethanol supports the existence of the pure host compound. Unlike this behaviour only a few weak reflections originating from pure Ph_3COH emerge from

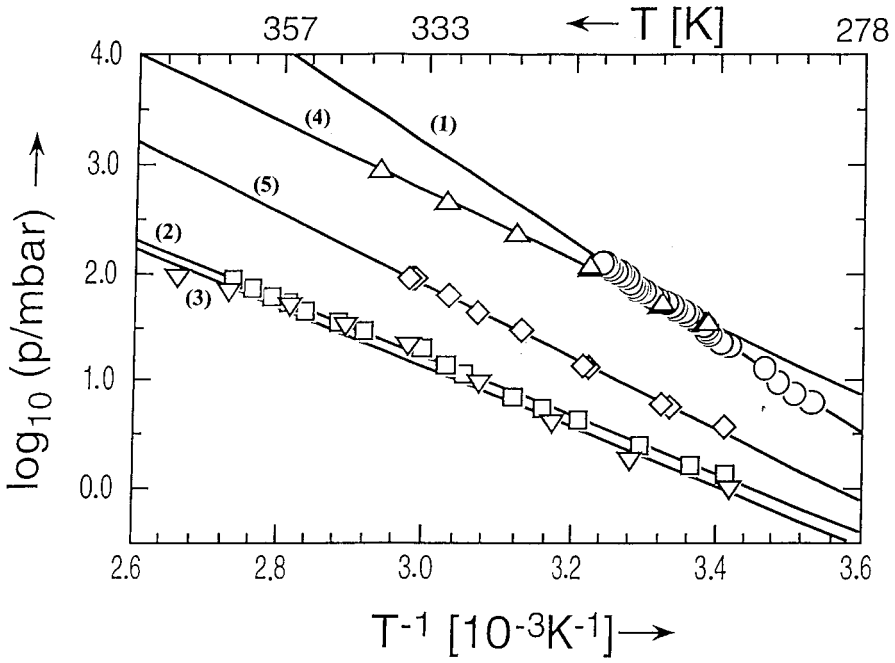

Figure 10. Plots of the vapor pressures $\log_{10} p_{(T)}$ of the compounds (**1**)–(**5**).

the high background at elevated temperatures for the compounds with DMF and dioxane. Here, the inclusion compounds decompose and melt in one step, but this process is not complete and a residue of pure crystalline host remains to melt at higher temperatures. This explains why only a small melting peak for triphenylmethanol is detected for (**5**) in the DTA. In the powder diffraction experiment the DMSO clathrate shows a well defined melting point as also observed in DTA, too. The temperatures of guest release deduced from powder diffraction correspond quite well with those determined by DTA; discrepancies can be explained by different experimental conditions like slower heating rates and narrowed sample tubes for the first method.

Vapor pressures. From the logarithmic plots of the vapor pressures of clathrates (**1**)–(**5**) versus reciprocal temperature in Figure 10 the equations of the resulting straight lines were derived and given in Table V for each inclusion compound. The heats of vaporization ΔH_v were determined from their slopes and are also listed in Table V together with the ΔH_v values for the pure solvents from the literature [18–20].

The heats of vaporization for all inclusion compounds except DMSO are higher than the corresponding values for the pure solvents. Thus, the guest molecules experience stronger interactions in the clathrate than in the liquid, mainly arising from hydrogen bonds between guest and host molecules. Only methanol and DMF

Table V. Results of the vapor pressure measurements. For comparison the numerical data for the pure solvents (liquid state) from literature are also given. ΔT is the temperature range of the measurement, ΔH_v the heat of vaporization.

Compound	Equation for the straight line $\log_{10} p_{(T)}$	ΔH_v (kJ mol^{-1})	ΔT (K)
(**1**)	$\log_{10}(p/\text{mbar}) = 16.40–4414.3 \cdot \text{T}^{-1} \cdot \text{K}$	84.45	283–309
Acetone		31.51	
(**2**)	$\log_{10}(p/\text{mbar}) = 9.34–2710.3 \cdot \text{T}^{-1} \cdot \text{K}$	51.88	293–366
DMSO		52.51	
(**3**)	$\log_{10}(p/\text{mbar}) = 12.15–3134.6 \cdot \text{T}^{-1} \cdot \text{K}$	52.60	292–376
DMF		43.25	
(**4**)	$\log_{10}(p/\text{mbar}) = 9.36–2747.5 \cdot \text{T}^{-1} \cdot \text{K}$	60.01	295–340
Methanol		37.89	
(**5**)	$\log_{10}(p/\text{mbar}) = 11.84–3322.2 \cdot \text{T}^{-1} \cdot \text{K}$	63.60	310–335
1,4-Dioxane		35.77[20]	

are able to form such hydrogen bonds in their liquid phases. It is known that DMSO molecules form chain-like associates $\cdots S(CH_3)_2O \cdots S(CH_3)_2O \cdots$ in the liquid at room temperature [13] with interactions between sulphur and oxygen atoms that are probably a little stronger than the hydrogen bonds between host and guest in the clathrate (**2**). Comparing the vapor pressures of inclusion compounds (**1**)–(**5**) one finds decreasing values in the sequence acetone $\approx$ methanol $>$ dioxane $>$ DMF $\approx$ DMSO. The values for the pure liquid solvents decrease in the same order, and therefore a relation between the vapor pressures of the inclusion compounds and the corresponding pure solvent must be taken into account.

Acknowledgements

The authors are grateful to the “Deutsche Forschungsgemeinschaft” for support of the work. Support of the “Fonds der Chemischen Industrie” is also acknowledged. R. I. is grateful to the Ministry of Education, Science and Culture, Japan, for the Grant-in-Aid for Scientific Research No. 06453055.

References

1. J. F. Norris: *J. Am. Chem. Soc.* **38**, 702 (1916).
2. E. Weber, K. Skobridis, and I. Goldberg: *J. Chem. Soc., Chem. Commun.* 1195 (1989).
3. S. A. Bourne, L. Johnson, C. Marais, L. R. Nassimbeni, E. Weber, K. Skobridis, and F. Toda: *J. Chem. Soc. Perkin Trans. 2*, 1707 (1991).
4. E. Weber, K. Skobridis, A. Wierig, and I. Goldberg: *J. Incl. Phenom.* **28**, 163 (1997).
5. K. Eckardt: PhD Thesis, University of Technology, Darmstadt, Germany (1996).
6. K. Eckardt, H. Fuess, R. Ikeda, H. Ohki, and Al. Weiss: *Z. Naturforsch.* **50a**, 758 (1995).

7. G. M. Sheldrick: SHELXS86. *Program for the Solution of Crystal Structures*, University of Göttingen, Germany, 1986. SHELXL93. *Program for Crystal Structure Determination*, University of Göttingen, Germany, 1993.
8. R. Strauss: PhD Thesis, University of Technology Darmstadt, Germany (1996).
9. G. Ferguson, J. F. Gallagher, C. Glidewell, J. N. Low, and S. N. Scrimgeour: *Acta Crystallogr.* **C48**, 1272 (1992).
10. A. Bondi: *J. Phys. Chem.* **68**, 441 (1964).
11. R. Basaran, S. Dou, and Al. Weiss: *Struct. Chem.* **4**, 219 (1993).
12. J. Seelig: *Quart. Rev. Biophys.* **10**, 353 (1977).
13. R. G. Barnes: *Advances in Nuclear Quadrupole Resonance*; Vol. 1, Heyden & Sons Ltd., p. 335 (1974).
14. R. Ikeda, A. Kubo, and C. A. McDowell: *J. Phys. Chem.* **93**, 7315 (1989).
15. L. W. Jelinski: *Annu. Rev. Mater. Sci.* **15**, 359 (1985).
16. *Ullmann's Encyclopedia of Industrial Chemistry*, 5th edn, Verlag Chemie, Weinheim (1985).
17. R. H. Smith and D. H. Andrews: *J. Am. Chem. Soc.* **53**, 3644 (1931).
18. J. Timmermans: *Physico-chemical Constants of Pure Organic Compounds*, Elsevier, Amsterdam (1950).
19. A. Delzenne: *Chem. Eng. Sci.* **2**, 220 (1953).
20. D. Stull: *Ind. Eng. Chem.* **39**, 517(1947).